Hindawi Publishing Corporation
International Journal of Distributed Sensor Networks
Volume 2015, Article ID 670216, 8 pages
http://dx.doi.org/10.1155/2015/670216

Research Article

Image Denoising Based on Improved Wavelet Threshold Function for Wireless Camera Networks and Transmissions

Xiaoyu Wang,[1] Xiaoxu Ou,[1] Bo-Wei Chen,[2] and Mucheol Kim[3]

[1]*School of Computer Science and Technology, Harbin University of Science and Technology, P.O. Box 261, No. 52 Xuefu Road, Harbin 150080, China*
[2]*Department of Electrical Engineering, National Cheng Kung University, No. 1, University Road, Tainan City 70101, Taiwan*
[3]*Department of Multimedia, Sungkyul University, No. 53, Manan-gu, Anyang City, Gyeonggi-do 430742, Republic of Korea*

Correspondence should be addressed to Xiaoyu Wang; xiaoyu_wang_hust@163.com

Received 11 August 2014; Accepted 31 August 2014

Academic Editor: Seungmin Rho

A new wavelet threshold denoising function and an improved threshold are proposed. It not only retains the advantages of hard and soft denoising functions but also overcomes the disadvantages of the continuity problem of hard denoising function and the constant deviation of the soft denoising function in the new method. In the case of the improved threshold conditions, the new threshold function has a better performance in outstanding image details. It can adapt to different images by joining an adjusting factor. Simulation results show that the new threshold function has a better ability of performing image details and a higher peak signal to noise ratio (PSNR).

1. Introduction

In the process of image transmission, the image is likely to be affected by noise in all aspects of transmission [1]. Due to these effects, the image will be interfered by noise. The visual effects of image are poor because of low image quality. At this point, the main noise in image transmission is the Gaussian noise. Fingerprint recognition, face recognition, and medical image are in great need of the image details, but a great interference to the image is brought by the image noise. These interferences are also promoting the development of the image denoising technology. Accuracy of minutiae extraction is very important in the automatic fingerprint identification technology based on matching minutiae [2]. Therefore, it is particularly important to preserve image details while removing the noise [3, 4]. The geometric method is the earliest and most traditional one for face detection and recognition. It usually needs to detect facial features, the relative position between the important facial features, and the relevant parameters of these features [5]; this method is badly in need of the detail information of the image. Image noise makes the image quality change so that it is difficult to extract the image feature. Image denoising can not only improve the practicability of the fingerprint, face recognition, and medical imaging but also enhance the visual effect of the image. The algorithm in this paper mainly aims at Gaussian noise.

Image denoising algorithms can be divided into spatial domain algorithm and frequency domain algorithm [6–9]. Spatial domain algorithm is to process the image pixels directly. In the frequency domain algorithm, the image is transformed from time domain to frequency domain. Then the image is processed in frequency domain and transformed to that in time domain. Mean filtering, median filtering, and adaptive Wiener filtering are classical spatial domain algorithms. It also caused some problems while removing the noise in these methods, such as serious blur of the image, especially the edge and details of the image [10]. Fourier transform is in common use in frequency domain; however, the domain characteristics of it disappeared after Fourier transform. It can neither detect the time position and the degree of intensity after signal transformation nor describe the local properties of time domain of the image [11]. The emergence and improvement of wavelet transform theory solves this problem. So wavelet has been widely used in image processing [12, 13].

Wavelet denoising algorithms can basically be divided into three categories: (1) modulus maxima algorithm based on wavelet transform [14]; (2) correlation algorithm [15]; (3) wavelet threshold algorithm [16, 17], including the hard threshold and soft threshold.

In the process of image denoising, the selection of threshold and the construction of threshold function are the keys to denoising. A new threshold and a new construction of threshold function are proposed in this paper. The new threshold and the new threshold function are used to obtain a higher value of the peak signal of noise ratio while more image details are retained.

2. Wavelet Threshold Principle

2.1. Wavelet Transforms in Two Dimensions. An image can be thought of as a two-dimensional function; then the wavelet transform of an image is a two-dimensional wavelet transform. A two-dimensional scaling function $\varphi(x, y)$ and three two-dimensional wavelets $\psi^H(x, y)$, $\psi^V(x, y)$, and $\psi^D(x, y)$ are needed in two-dimensional wavelet transform. Each two-dimensional function above is the result of multiplying one-dimension function φ and ψ. Excluding the product of one-dimensional results, the remaining products produced a separable scaling function

$$\varphi(x, y) = \varphi(x)\varphi(y) \tag{1}$$

and separable "directionally sensitive" wavelets

$$\begin{aligned} \psi^H(x, y) &= \psi(x)\varphi(y), \\ \psi^V(x, y) &= \varphi(x)\psi(y), \\ \psi^D(x, y) &= \psi(x)\psi(y). \end{aligned} \tag{2}$$

These wavelets measure variations of the function of an image, the intensity variations for images along the gray level of different directions. ψ^H measures variations along columns (e.g., horizontal edges), ψ^V responds to variations along rows (like vertical edges), and ψ^D corresponds to variations along diagonals [18].

Given separable two-dimensional scaling and wavelet functions, then the two-dimensional wavelet transform becomes very simple. Firstly, we give a scaling function and a translated basis function:

$$\begin{aligned} \varphi_{j,m,n}(x, y) &= 2^{j/2}\varphi\left(2^j x - m, 2^j y - n\right), \\ \psi^i_{j,m,n}(x, y) &= 2^{j/2}\psi^i\left(2^j x - m, 2^j y - n\right), \quad i = \{H, V, D\}. \end{aligned} \tag{3}$$

Here, i is the directional wavelets in above "directionally sensitive" wavelets (H represents the horizontal direction, V represents the vertical direction, and D represents the diagonal direction). j controls the width of $\varphi_{j,m,m}(x, y)$, and the term $2^{j/2}$ controls the amplitude of $\varphi_{j,m,m}(x, y)$. m and n determine the position of $\varphi_{j,m,m}(x, y)$ along x-axis and y-axis. The discrete wavelet transform for two-dimensional image $f(x, y)$ of size $M \times N$ is

$$\begin{aligned} W_\varphi(j_0, m, n) &= \frac{1}{\sqrt{MN}} \sum_{x=0}^{M-1} \sum_{y=0}^{N-1} f(x, y)\varphi_{j_0,m,n}(x, y), \\ W^i_\psi(j, m, n) &= \frac{1}{\sqrt{MN}} \sum_{x=0}^{M-1} \sum_{y=0}^{N-1} f(x, y)\psi^i_{j,m,n}(x, y) \\ & \qquad i = \{H, V, D\}. \end{aligned} \tag{4}$$

j_0 is the arbitrary initial scale of the scaling function and the coefficients of $W^i_\psi(j, m, n)$ can be considered the approximation of $f(x, y)$ at scale j_0. The coefficients of $W^i_\psi(j, m, n)$ add details of horizontal, vertical, and diagonal for $j \geq j_0$. In the $W^i_\psi(j, m, n)$ function, we usually let $j_0 = 0$ and select $N = M = 2^J$. Then we can know $j = 0, 1, 2, \ldots, J - 1$ and $m, n = 0, 1, 2, \ldots, 2^j - 1$. $f(x, y)$ can be obtained via the inverse discrete wavelet transform while the W_φ and W^i_ψ are given. Consider

$$\begin{aligned} & f(x, y) \\ &= \frac{1}{\sqrt{MN}} \sum_m \sum_n W_\varphi(j_0, m, n)\varphi_{j_0,m,n}(x, y) \\ &\quad + \frac{1}{\sqrt{MN}} \sum_{i=H,V,D} \sum_{j=j_0}^{\infty} \sum_m \sum_n W^i_\psi(j, m, n)\psi^i_{j,m,n}(x, y). \end{aligned} \tag{5}$$

We can use Figure 1 [18] to represent two-dimensional wavelet transform and use Figure 2 [18] to represent its inverse transform.

Four coefficient matrices can be obtained by the first wavelet transform of an image; one is the coefficient matrix of low frequency by the scaling function expansion and the other three coefficient matrices are generated by the translated basis functions. Wavelet threshold denoising is to modify these four coefficient matrices with a threshold and then use the four coefficient matrices after modification to reconstruct the image.

2.2. Wavelet Threshold Principle. Donoho and Johnstone proposed the theory of wavelet threshold shrinkage in 1992; the main theoretical basis of this theory is as follows [16, 19, 20]. The energy distribution of the signal in Besov space is mainly concentrated in the limited coefficients in wavelet domain, whereas the noise's energy is distributed throughout the wavelet domain. Therefore, the transform coefficients of signal are greater than that of noise after wavelet decomposition. We can find a suitable threshold. When the amplitudes of wavelet coefficients are less than the preset threshold, it is considered that the amplitude is caused by the noise and the amplitude is set to zero; when the amplitudes of wavelet coefficients are greater than the threshold, it is considered that the amplitude is caused by signal and the amplitude is preserved or revised. The image is reconstructed by the processed wavelet coefficients in the

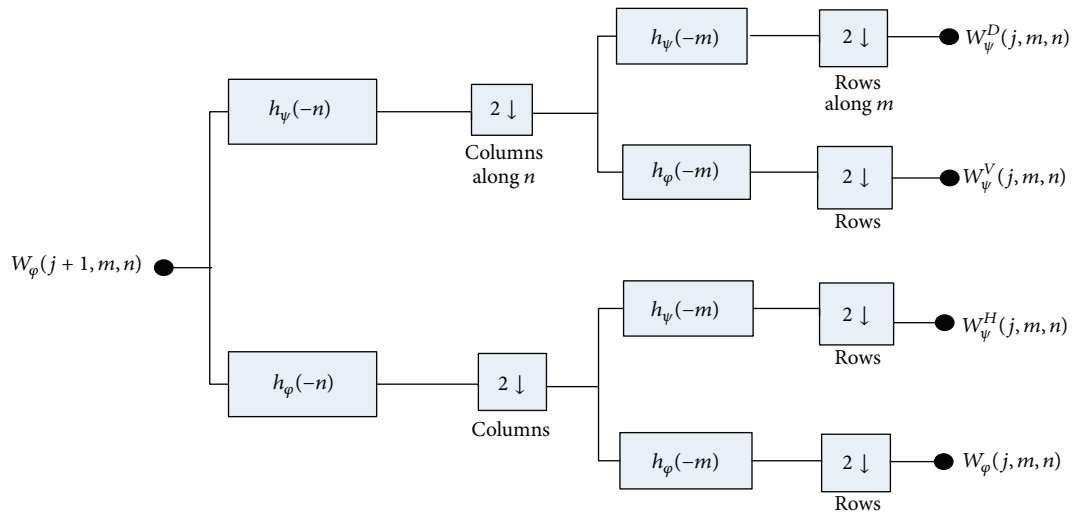

Figure 1: The discrete wavelet transform. Here, $h_\psi(-n)$, $h_\psi(-n)$, $h_\psi(-m)$, and $h_\varphi(-m)$ are wavelet vectors. 2 ↓ represents downsampling by 2.

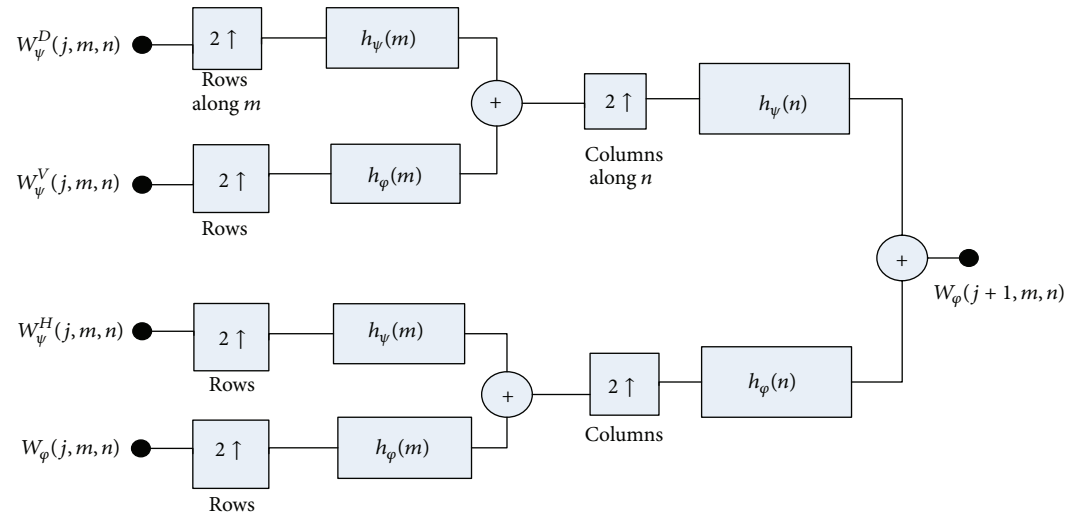

Figure 2: The inverse discrete wavelet transform. Here, $h_\psi(m)$, $h_\varphi(m)$, $h_\psi(n)$, and $h_\varphi(n)$ are wavelet vectors. 2 ↑ signifies upsampling by 2.

steps above to achieve the purpose of image denoising. This algorithm is simple, has better visual effects, and can keep the edge information.

Assume that the original image is s_{ij}; the model of the noise image is

$$f_{ij} = s_{ij} + n_{ij}, \tag{6}$$

where f_{ij}, s_{ij}, and n_{ij} represent the noise image, the original image, and the corrupting white Gaussian noise, respectively. $i, j = 1, 2, 3 \ldots N$, N is an integer power of 2.

The steps of wavelet threshold denoising are as follows from the analysis above.

(1) Select a suitable wavelet base and decomposition levels to decompose the image f_{ij}, and the wavelet coefficient of the noise image is w_{ij}. Here, the input is f_{ij} and the output is w_{ij}.

(2) Select an appropriate threshold to process the high frequent wavelet coefficients of the noise image in each layer, and obtain the new coefficients $\widehat{w}_{ij}$. Here, the input is w_{ij} and the output is $\widehat{w}_{ij}$.

(3) Reconstruct the image with the original low frequency wavelet coefficients and $\widehat{w}_{ij}$ to get the denoising image. Here, the inputs are the original low frequency wavelet coefficients and $\widehat{w}_{ij}$. And the final output is the denoising image.

3. Wavelet Threshold Denoising Function

3.1. Several Common Denoising Threshold Functions

(1) The hard threshold denoising function.

The function is

$$\widehat{w}_{ij} = \begin{cases} w_{ij}, & \left|w_{ij}\right| > \lambda \\ 0, & \left|w_{ij}\right| \le \lambda, \end{cases} \tag{7}$$

where w_{ij}, λ represent the wavelet coefficients of the noisy image and the threshold, respectively, and $\widehat{w}_{ij}$ is the result of the wavelet coefficients processed by the hard threshold function.

(2) The soft threshold denoising function.

The function is

$$\widehat{w}_{ij} = \begin{cases} \operatorname{sgn}\left(w_{ij}\right)\left(\left|w_{ij}\right| - \lambda\right), & \left|w_{ij}\right| > \lambda \\ 0, & \left|w_{ij}\right| \le \lambda, \end{cases} \tag{8}$$

where w_{ij}, λ represent the wavelet coefficients of the noisy image and the threshold, respectively, and $\widehat{w}_{ij}$ is the result of the wavelet coefficients processed by the soft threshold function. $\operatorname{sgn}(w_{ij})$ represents the sign of w_{ij}.

(3) The improved soft threshold denoising function.

The function is

$$\widehat{w}_{ij} = \begin{cases} \operatorname{sgn}\left(w_{ij}\right)\left(\left|w_{ij}\right| - \alpha\lambda\right), & \left|w_{ij}\right| > \lambda \\ 0, & \left|w_{ij}\right| \le \lambda, \end{cases} \tag{9}$$

where w_{ij}, λ represent the wavelet coefficients of the noisy image and the threshold, respectively, and $\widehat{w}_{ij}$ is the result of the wavelet coefficients processed by the improved soft threshold denoising function. $\operatorname{sgn}(w_{ij})$ represents the sign of w_{ij} and α $(0 < \alpha < 1)$ is an adjustment factor of λ.

(4) The semisoft threshold denoising function.

The function is

$$\widehat{w}_{ij} = \begin{cases} w_{ij}, & \left|w_{ij}\right| > \lambda_2 \\ \operatorname{sgn}\left(w_{ij}\right)\dfrac{\lambda_2\left(\left|w_{ij}\right| - \lambda_1\right)}{\lambda_2 - \lambda_1}, & \lambda_1 \le \left|w_{ij}\right| \le \lambda_2 \\ 0, & \left|w_{ij}\right| < \lambda_1, \end{cases} \tag{10}$$

where w_{ij}, $\operatorname{sgn}(w_{ij})$ represent the wavelet coefficients of the noisy image and the sign of w_{ij}, respectively, and $\widehat{w}_{ij}$ is the result of the wavelet coefficients processed by the soft threshold function. λ_1, λ_2 are the thresholds of this function. The images of all the functions above are shown in Figure 3.

The soft threshold function and hard threshold function of Donoho have been widely used, but it remains inadequate. The edges of the image are blurred because the wavelet coefficients of the noisy image that are greater than the threshold are shrunk in the soft threshold denoising function [21]. The hard threshold denoising function can keep the local information of the image. However, the image will show the visual distortion caused by pseudo Gibbs phenomena because the hard threshold denoising function is not continuous at the threshold [22]. In addition, highlighting the details of the image is not particularly obvious in the hard threshold and soft threshold denoising function. A new threshold function will be introduced in the following paper.

3.2. The Improved Wavelet Threshold Function. The new function is

$$\widehat{w}_{ij} = \begin{cases} \operatorname{sgn}\left(w_{ij}\right)\left[\left|w_{ij}\right| - \sin\left(\dfrac{\pi}{2}\left|\dfrac{\lambda}{w_{ij}}\right|^n\right)\lambda\right], & \left|w_{ij}\right| > \lambda \\ 0, & \left|w_{ij}\right| > \lambda, \end{cases} \tag{11}$$

where w_{ij}, λ represent the wavelet coefficients of the noisy image and the threshold, respectively, and $\widehat{w}_{ij}$ is the result of the wavelet coefficients processed by the new threshold function. $\operatorname{sgn}(w_{ij})$ represents the sign of w_{ij}. And n is an adjustment parameter.

In the new threshold function, if $|w_{ij}| \to \lambda$, the value of $\widehat{w}_{ij} \to 0$. We can know that the new function is continuous at the threshold point so that the pseudo Gibbs phenomena can be avoided. If $|w_{ij}| \to \infty$, the value of $\widehat{w}_{ij} \to w_{ij}$. It can be seen that when w_{ij} is larger, the difference between w_{ij} and $\widehat{w}_{ij}$ becomes smaller gradually. It can solve the problem of fixed deviation brought by the soft threshold function, and the edge blur of the image can be degraded. n can be adjusted depending on the different thresholds of the different images to make the new function adapt to more images. The image of the improved function is shown in Figure 3.

4. Matlab Simulation Experiment and Results

4.1. Simulation Experiment. In order to show the superiority of the proposed algorithm, soft threshold and hard threshold denoising were selected as contrast. In this section, simulated experiments are performed with "kids.tif," "mir.tif" (a medical image), and "105_7.tif" (an image in FVC2004 fingerprint database). This experiment has been performed using Matlab programming language (Matlab R2012b). The specific experimental steps are as follows.

(1) Add Gaussian white noise that the mean is 0 and the variance is 0.01 into the selected images.

(2) Decompose all the noisy images with wavelet base "sym4" to obtain the wavelet coefficients of each layer of all the images.

(3) Denoise the noisy images with the soft and hard threshold denoising method.

(4) Denoise the noisy images with the improved denoising method in this paper.

(5) Reconstruct image with the wavelet coefficients processed by soft, hard, and the new threshold denoising method, and compare the performance of the three methods.

(6) Use the peak signal to noise ratio (PSNR) as the evaluation criteria to evaluate each algorithm. Here, PSNR is defined as

$$\mathrm{PSNR} = 10\lg\left(\frac{f_{\max}^2}{(1/MN)\sum_{i=0}^{M-1}\sum_{j=0}^{N-1}\left[f(i,j) - f_0(i,j)\right]^2}\right), \tag{12}$$

where $f_{\max}$ is the maximum gray level of the image, M and N denote the size of the image, $f(i, j)$ is the restored image, and $f_0(i, j)$ is the original image.

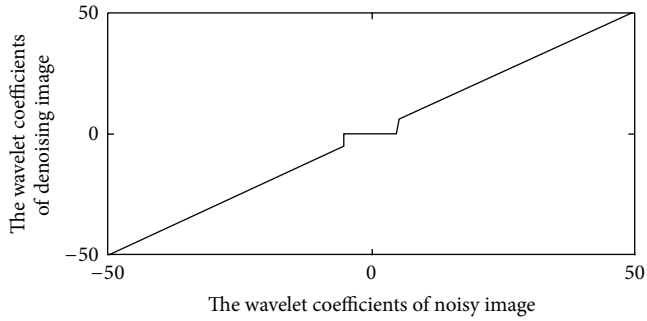

(a) The hard threshold denoising function

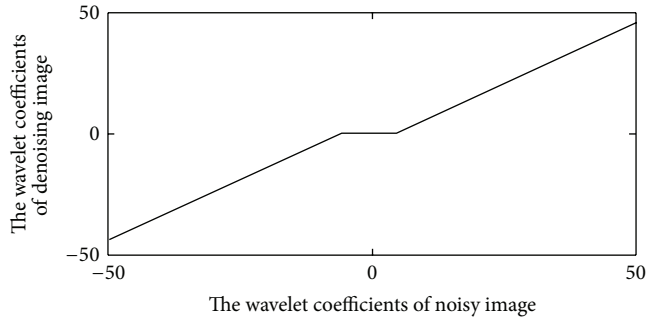

(b) The soft threshold denoising function

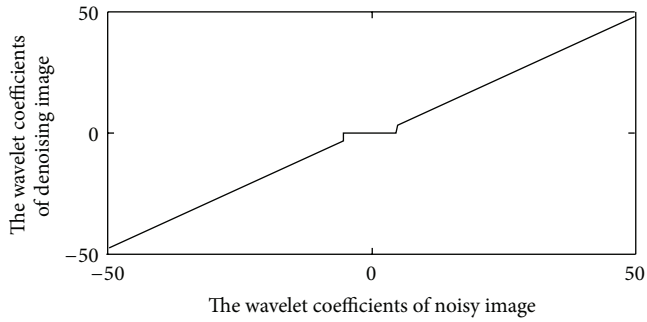

(c) The improved soft threshold denoising function

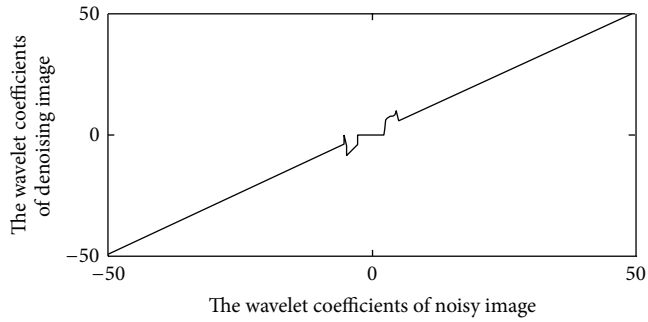

(d) The semisoft threshold denoising function

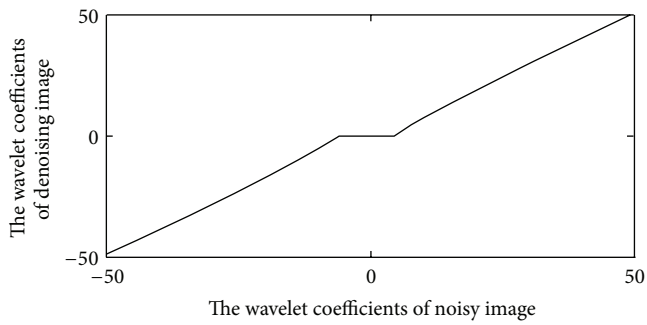

(e) The improved wavelet threshold function

Figure 3: The images of threshold denoising functions above.

Table 1: Comparison of PSNR (dB): kids.tif.

Variance of Gaussian noise	0.01	0.03	0.05
Result of hard threshold	31.7121	27.6174	26.3008
Result of soft threshold	33.7362	29.2526	27.3461
Result of improved algorithm	34.2701	29.7518	28.0052

Table 2: Comparison of PSNR (dB): mir.tif.

Variance of Gaussian noise	0.01	0.03	0.05
Result of hard threshold	28.3733	25.6540	25.2654
Result of soft threshold	28.8702	26.6270	26.2286
Result of improved algorithm	29.9496	26.7387	25.9008

Table 3: Comparison of PSNR (dB): 105_7.tif.

Variance of Gaussian noise	0.01	0.03	0.05
Result of hard threshold	35.4000	34.6260	34.1692
Result of soft threshold	35.5536	35.1307	35.1261
Result of improved algorithm	36.4919	35.5582	35.1889

4.2. Experimental Results. The original image, noisy image, and the image after denoising processing are shown in Figure 4.

Local enlarged images of denoising images are shown in Figure 5.

We set $n = 0.02$ for the improved threshold denoising function in the simulation experiment. PSNR of the different variance for these 3 images are shown in Tables 1, 2, and 3.

4.3. Selection of Threshold. Selecting the threshold is critical in the wavelet threshold denoising method. The suitability of

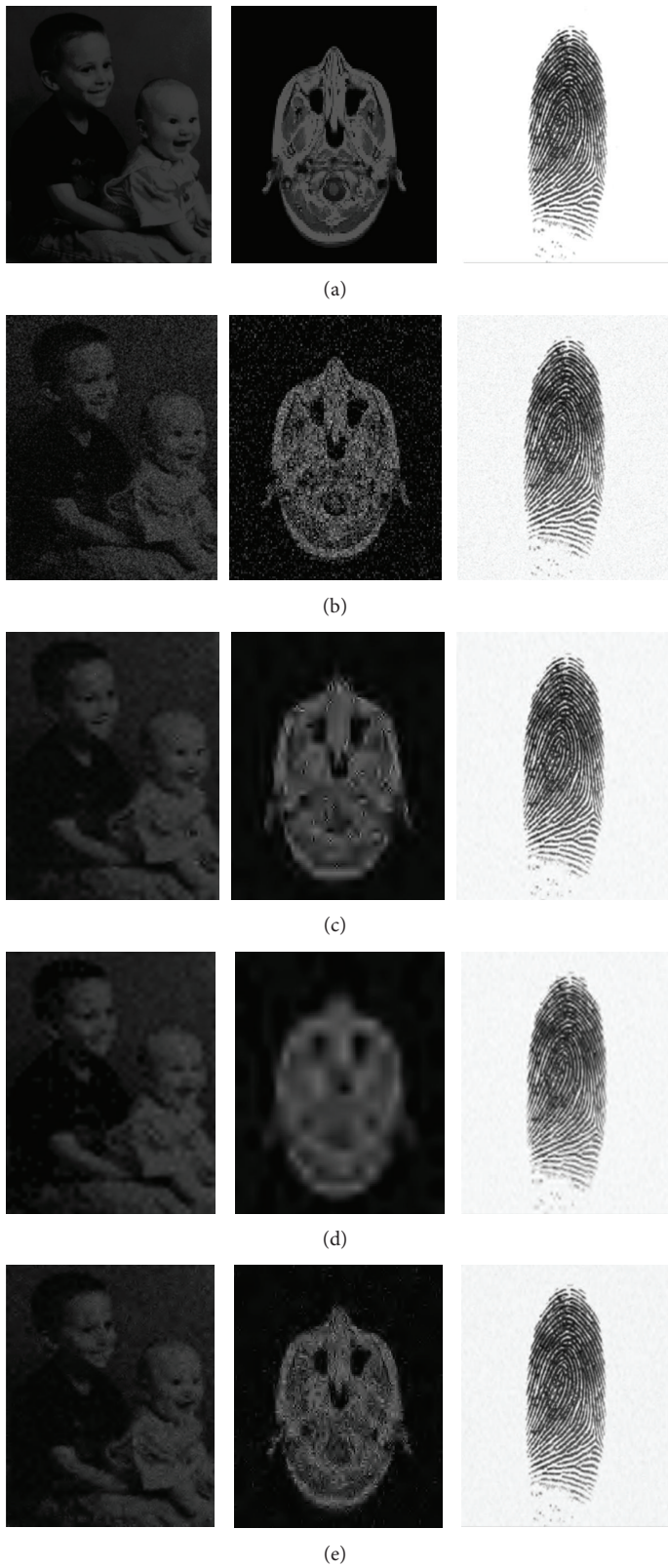

Figure 4: Images denoising. (a) Original image. (b) Image corrupted by Gaussian white noise that the mean is 0 and the variance is 0.01. (c) The denoising result of hard threshold. (d) The denoising result of soft threshold. (e) The denoising result of improved algorithm.

(a)

(b)

(c)

Figure 5: Local enlarged denoising images. (a) The hard threshold denoising algorithm. (b) The soft threshold denoising algorithm. (c) The improved wavelet threshold algorithm.

it affects the denoising effect of image directly. In the VisuShrink algorithm proposed by Donoho, Universal threshold expression [19] is $\lambda = \delta\sqrt{2\ln(N)}$, where N represents the length of the signal; $\delta = \text{median}(|w_{ij}|)/0.6745$, $w_{ij} \in HH_1$, and HH_1 is the diagonal coefficients of the first layer of wavelet decomposition for the noisy image.

The threshold value used in this paper is a modification of [2]. The threshold expression in [2] is $\lambda = \delta\sqrt{2lb(m)}/j$, where δ, m, and j represent a standard deviation of the noisy image, the total number of wavelet coefficients of the image, and the level of decomposition. The noise amplitude is smaller and smaller while the signal amplitude is larger and larger with the increasing of decomposition levels of the noisy image. The threshold expression used in this paper is $\lambda_j = \delta_j\sqrt{2lb(m)}/(j+2)$, where λ_j, m, and j represent the threshold of level j after wavelet decomposition of the noisy image, the total number of wavelet coefficients of the image, and the level of decomposition. Here, $\sigma_j = \text{median}(|w_{ij}|)/0.6745$, where w_{ij} is the high frequency coefficients of the horizontal, vertical, and diagonal directions of layer j.

5. Conclusion

Wavelet transform has a good time-frequency characteristics. Because the frequency distributions of noise and image signal are different, wavelet transform for image denoising has obvious advantages. In this paper, we proposed a new threshold function to improve inadequacies of the soft threshold and hard threshold based on the original threshold function by analyzing the characteristics of wavelet threshold function. Under different noise conditions, the new threshold function can retain more image details and get a higher PSNR. Improved threshold denoising function has a good application prospect in the face and fingerprint denoising and medical imaging denoising.

Conflict of Interests

The authors declare that there is no conflict of interests regarding the publication of this paper.

Acknowledgment

This work is supported by the Project of Education Department of Heilongjiang Province (Grant no. 12541177).

References

[1] C. Qin, Z. Chen, K. Yu, and Y. Zhou, "Research on JPEG2000-based rate control algorithm," *Computer Applications and Software*, vol. 28, no. 2, pp. 253–255, 2011.

[2] Y. Huang and D. Hou, "Fingerprint de-noising based on improved wavelet threshold function," *Computer Engineer and Applications*, vol. 50, no. 6, pp. 179–181, 2014.

[3] N. Yanmin and W. Xuchu, "Statistical modeling of nonsubsampled contourlet transform coefficients and its application to image denoising," *Laser & Optoelectronics Progress*, vol. 47, no. 5, Article ID 051005, 5 pages, 2010.

[4] J. Peng, S. Liu, and L. An, "The new variable step size LMS adaptive filtering algorithm for low SNR," *Chinese Journal of Sensors and Actuators*, vol. 26, no. 8, pp. 1116–1120, 2013.

[5] J.-Y. Wu and D.-L. Zhou, "Survey of face recognition," *Application Research of Computers*, vol. 26, no. 9, pp. 3205–3209, 2009.

[6] Z. Jia, S. Hui, D. Cheng-Zhi, and C. Xi, "Particle swarm optimization based adaptive image denoising in shearlet domain ," *Journal of Chinese Computer Systems*, vol. 32, no. 6, pp. 1147–1150, 2011.

[7] N.-F. Yang, C.-M. Wu, and H.-Z. Qu, "Mixed noised denoised based on partial differential equation," *Application Research of Computers*, vol. 30, no. 6, pp. 1899–1902, 2013.

[8] Y. Zhang, P. Zhang, G. Wang, and H. Zhuo, "Denoising method for color images based on chrominance model and curvelet transform," *Journal of Image and Graphics*, vol. 17, no. 12, pp. 1472–1477, 2012.

[9] L. Zhang and X. Li, "Image denoising method of partial differential equation based on wavelet transform," *Laser & Infrared*, vol. 43, no. 8, pp. 943–946, 2013.

[10] J. Yang, C. Wu, and H. Qu, "Multi-parameter threshold function for image de-noising based on wavelet transform," *Computer Engineering and Applications*, vol. 48, no. 13, pp. 176–180, 2012.

[11] Q. Wang, L.-Y. Gong, W.-J. Ren, F.-C. Huo, and F. Gao, "The algorithm of image denoising based on the improved method of wavelet thresholding," *Techniques of Automation & Applications*, vol. 32, no. 11, pp. 61–66, 2013.

[12] X. U. Jing, F. U. Wei, H. U. Cai-Ning, and W. U. Hua, "Implementation of improved embedded Zerotree wavelet image coding algorithm," *Radio Communications Technology*, vol. 34, no. 5, pp. 62–64, 2008.

[13] L. Zhai and L. Zhao, "Adaptive image watermarking algorithm based on wavelet packet transform," *Radio Engineering*, vol. 43, no. 2, pp. 23–26, 2013.

[14] S. Mallat and S. Zhong, "Characterizating of singnal from multiscale edges," *IEEE Transactions on Pattern Analysis and Machine Intelligence*, vol. 14, no. 7, pp. 710–732, 1992.

[15] H. X. Yang, X. S. Wang, P. H. Xie, A. Leng, and Y. Peng, "Infrared image denoising based on improved threshold and inter-scale correlations of wavelet transform," *Acta Automatica Sinica*, vol. 37, no. 10, pp. 1167–1174, 2011.

[16] D. L. Donoho, "De-noising by soft-thresholding," *IEEE Transactions on Information Theory*, vol. 41, no. 3, pp. 613–627, 1995.

[17] M. U. Juan, D. U. Chao-Ben, and Y. I. Zhou, "Adaptive threshold for remote sensing image denoising based on wavelet and NSCT," *Radio Engineering*, vol. 42, no. 11, pp. 23–25, 2012.

[18] R. C. Gonzalez and R. E. Woods, *Digtal Image Processing*, Publishing House of Electronics Industry, Beijing, China, 3rd edition, 2010.

[19] D. L. Donoho and I. M. Johnstone, "Ideal spatial adaptation by wavelet shrinkage," *Biometrika*, vol. 81, no. 3, pp. 425–455, 1994.

[20] Y. Zhao and T. A. Turki, "Denoising method of wavelet threshold function improvement," *Computer Engineering and Applications*, vol. 49, no. 22, pp. 212–214, 2013.

[21] C. Biao, *Study on Image Denoising and Texture Classifiaction Based on Wavelet Theory*, Heifei University of Technology, Hefei, China, 2008.

[22] G. Wen-zhong, C. Zhi-yun, and Z. Qiu-mei, "Improved algorithm of wavelet thresholding for image denoising," *Journal of East China Normal University (Natural Sciences)*, vol. 2013, no. 6, pp. 83–92, 2013.